Reducing Electromagnetic Coupling in Shielded Enclosures using a Genetic Algorithm – Finite-Difference Time-Domain Solver

Russell Iain Macpherson[1] and Nick J Ryan[2]
Department of Engineering
King's College
University of Aberdeen
Aberdeen AB24 3UE
United Kingdom
r.macpherson@ieee.org[1], n.j.ryan@eng.abdn.ac.uk[2]

Abstract: Comprehensive shielding in modern electronic equipment may lead to resonant behaviour within the equipment enclosure. This paper presents a method for optimising the placement of sources of electromagnetic (EM) energy and susceptors to this EM energy within an enclosed resonant cavity. The source and susceptor are placed on a dielectric slab within a perfectly conducting enclosure to reduce the level of EM coupling between the two. Optimisation is facilitated using a genetic algorithm coupled with a finite-difference time-domain solver. Results are presented for single objective optimisation and multi-objective optimisation cases.

1 Introduction

The explosive increase in the use of electronic equipment in the information age has led to electromagnetic compatibility (EMC) and electromagnetic interference (EMI) issues becoming more important to designers of electronic equipment. These issues must be considered at the time of design and not once designs are at the prototype stage. Higher clock speeds and faster switching transitions lead to greater levels of electromagnetic emissions, while higher component integration and lower power demands lead to greater sensitivity. So at once systems are becoming more prone to generating and also more sensitive towards EMI.

An area of interest to the authors is electronic enclosures and the placement of devices inside these enclosures. Modern electronic items have many different sources of EMI. These sources are often placed inside a rectangular shaped metal box to limit the EM emissions from the equipment. Care is taken to ensure the shielding is as comprehensive as possible thus apertures are kept to a minimum and covered in metallic blanking plates. Such a shielded, rectangular enclosure has a good chance of forming a resonant cavity so that field strengths generated by the circuit may well be enhanced once the circuit is mounted within the casing. Normally the circuit may have a number of sources within the enclosure, all of which add to the EM fields within; changing the positions of the various sources will change the amount of resonance and constructive interference, [1]. There are also likely to be a number of susceptors at multiple locations throughout the circuit.

There is obviously an optimal size and shape of enclosure and component layout however, exhaustively placing components inside enclosures and then computing the resultant fields is a task that that would require a massive undertaking on behalf of the designer. A far better approach to component placement is to use some kind of optimisation method to place the components to achieve a desired radiation level. This paper describes the novel use of a genetic algorithm (GA) and a finite-difference time-domain (FDTD) solver to optimise source and susceptor placement inside a perfectly conducting structure, building upon initial work completed in [2].

Genetic algorithms are briefly introduced in section 2 and then the Finite-Difference Time-Domain method is introduced in section 3. Section 4 describes the setup of the computer simulation and section 5 discusses the results of these simulations, finally section 6 presents conclusions from the work.

2 Genetic Algorithms

GAs are a stochastic search mechanism with their operation firmly rooted in natural selection and survival of the fittest, [3] and [4]. GAs have been shown to provide robust search and optimisation in complex spaces, [3] and [5]. They use simple operations on a population of individuals, which lead to an emergent evolution of an individual or individuals. Each individual in the population represents a potential solution to the given problem scenario and as such is evaluated. After an individual has been evaluated a figure of merit (FoM) is attributed to the individual. This FoM is a measure of how well the individual solves the problem. GAs can lead to the optimal solution to a problem, more often however, they are used to optimise a problem towards an improved solution facilitating a trade-off between excessive computational time and meaningful results. The GA process can be summarised graphically as shown in figure 1.

The GA methodology used in this work is the micro genetic algorithm (μGA). The μGA technique has been shown to reach the optimal area of multi-modal solution spaces earlier than conventional GA methods, with min-

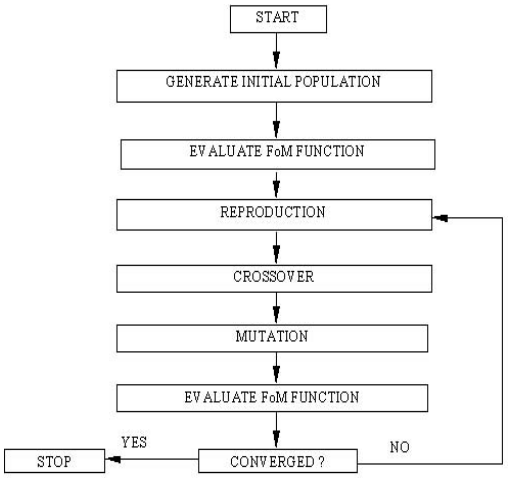

Figure 1: *GA Process Flowchart.*

imal computing time, [6]. It has already been demonstrated that the μGA can be successfully linked with an FDTD solver, [7], for optimisation in EM problems. Initially in a GA a fixed size population is created and populated with randomly generated individuals of a fixed length, this length is determined by the encoding of the problem parameters. The population size for the μGA is generally kept small *e.g.* five, this is different from the classic GA where the population size is typically much larger, in the order of 100s. These individuals are all possible solutions to the same given problem. They are assessed and each one given a score, the FoM, which is then used to determine the likelihood of reproduction into the next generation. The FoM is analogous to fitness in the natural world where fitter individuals survive longer and hence have a better chance of continuing their genetic lineage. The particularly successful, higher scoring individuals may be reproduced more than once into the next generation. In the μGA used here tournament selection is employed, this is perhaps the most effective for many application types as it has been shown to provide better convergence towards a solution in the initial stages of optimisation, [8]. Tournament selection works by randomly choosing N members of the population and in this instance as in many others $N = 2$. These individuals are then pitched against each other to determine which has the better FoM, the winner of the tournament being selected to be a member of the new population; this is repeated until the new population is filled. In conjunction with tournament selection elitist reproduction is also employed, this guarantees that the best individual from a population is present in the next population, hence preserving the best current solution to the given problem and maintaining a good genetic stock. After reproduction the individuals undergo crossover. Here two randomly picked individuals are mated together, swapping information between their chromosomes. In a classic GA mutation is also applied, however in the μGA mutation is turned off. Mutation serves to alter the genetic makeup of these new offspring with a small fixed probability. Once again mimicking nature, mutation can lead to either a detrimental or beneficial effect on performance. Mutation allows, in a classic GA, random search to take place and hopefully leads to the avoidance of local optima. Once the population has converged to a determined optimal value then further GA operating is no longer needed and the GA can be halted. Due to the small population size used in the μGA premature convergence is often seen to be happening, to prevent this a restart mechanism is used. This restart mechanism involves checking for convergence in the current generation of individuals and then restarting the next generation with only the elite individual and new randomly created individuals. The use of a restart operator ensures random search takes place and leads μGA away from local optima. Convergence is checked for in this application by measuring the changes in the chromosomes, the individuals, between generations. Once there are few changes between generations then the population can be considered to be converged, the setting of this limit is a parameter that the user has control over. An important component of any GA code is the device by which random numbers are generated, or to be more correct pseudo-random numbers. This is usually a portable pseudo-random number generator (PRNG) that produces the same sequence of *random* numbers for a given seed value. The *quality* of the PRNG is an important factor. The area of PRNG research is vast and not going to be, for brevity, discussed here. Common references on the subject are [9], [10], [11] and [12].

A clear difference can be seen here between optimisation based on calculus methods and GA based optimisation. GAs make use of interim performance in the optimisation problem, calculus based methods are only concerned with optimisation toward an overall optimal point and do not "remember" any interim performances.

3 The FDTD Method

The FDTD method, [13], [14], has become one of the most popular methods for solving Maxwell's equations. It is a volumetric domain decomposition technique that is second order accurate in space and time, easily implemented in software and accurately models the physical world. It is a widely used method for EMC/EMI work, [15], as well as radar, bioengineering and antenna analysis. The FDTD method is described widely in the literature, [16], and so only a very brief description is given here.

Maxwell's equations, in differential form, equations (1) - (2), are simply modified to central-difference equations, discretised, and implemented in software. The equations are solved in a leap-frog manner, [14], *i.e.* the electric field is solved at a given instant in time, then the magnetic field is solved at the next instant in time, and the process is repeated over and over again. In equations (1) and (2) $\boldsymbol{H}$ and $\boldsymbol{E}$ have their usual meanings.

$$\frac{\partial \boldsymbol{H}}{\partial t} = -\left(\frac{1}{\mu}\nabla \times \boldsymbol{E} + \frac{\rho'}{\mu}\boldsymbol{H}\right), \tag{1}$$

$$\frac{\partial \boldsymbol{E}}{\partial t} = \frac{1}{\epsilon}\nabla \times \boldsymbol{H} - \frac{\sigma}{\epsilon}\boldsymbol{E}. \tag{2}$$

Using a three dimensional Cartesian co-ordinate system we can now write out the vector components of the curl operator. Given below is only one of these components, namely the x component of the $\boldsymbol{H}$ field,

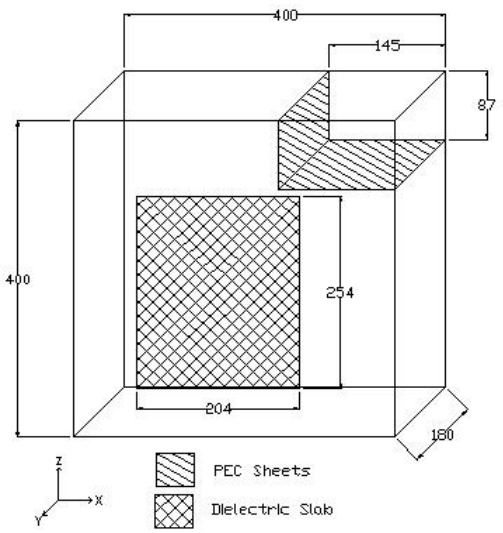

Figure 2: *Enclosure geometry showing the representations of the internal structure and dielectric slab, all sizes are in millimetres, mm.*

$$\frac{\partial H_x}{\partial t} = \frac{1}{\mu}\left(\frac{\partial E_y}{\partial z} - \frac{\partial E_z}{\partial y} - \rho' H_x\right), \tag{3}$$

where μ is magnetic permeability and ρ' is a magnetic loss parameter. It is the complete set of coupled partial differential equations, six in total, that are the fundamental basis of the numerical FDTD algorithm. The discretised form of equation (3) is shown below:

$$\begin{aligned} m &= MEDIA_{H_x|_{i,j,k}}, \\ H_x|_{i,j,k}^{n+\frac{1}{2}} &= D_a(m)\, H_x|_{i,j,k}^{n-\frac{1}{2}} \\ &+ D_b(m)\left(\begin{array}{c} E_y|_{i,j,k+\frac{1}{2}}^{n} - E_y|_{i,j,k-\frac{1}{2}}^{n} \\ +E_z|_{i,j-\frac{1}{2},k}^{n} - E_z|_{i,j+\frac{1}{2},k}^{n} \end{array}\right), \end{aligned} \tag{4}$$

where n is the time step under consideration and i, j, k are the three orthogonal spatial co-ordinates. The integer array MEDIA defines material conditions for each field vector component. This allows the medium at each point to be mapped out. The arrays D_a, D_b are magnetic field update coefficients, there are corresponding electric field update coefficients also. A full explanation of all of these equations is presented in [13].

4 Simulation Setup

The initial results are obtained from using the GA to place a source and susceptor point relative to each other on the surface of a dielectric slab (DS) to achieve the lowest electromagnetic coupling between the two. The complete simulation is implemented in Fortran 77 compiled on a SUN ENTERPRISE server with 512MB of RAM utilising 4 of 8 processors.

4.1 Physical Problem Description

The problem geometry is that of a simplified metal box, which has perfectly electrically conducting (PEC) walls, an internal structure and DS representation. The internal structure is modelled as two PEC sheets in the top corner of the geometry. The DS can be thought of as a representation of the substrate of a printed circuit board (PCB). The problem geometry is shown in figure 2. The DS has a relative permittivity, ϵ_r, of 4 and possesses unity magnetic permeability μ_r.

4.2 μGA and FDTD Setup

The μGA used is based on the implementation by Carroll, [17], modified to accommodate the given task of moving the source point and susceptor point on the DS. The two points are specified in a three dimensional Cartesian system with the y ordinate being held constant as this represents the surface of the DS. Binary encoding is used in the μGA and this leads to a chromosome string length of 24 bits, 4 bits per x, y and z co-ordinate of the source and susceptor. It should be noted that it would be possible to omit the y ordinate from the chromosome however the memory saving would be insignificant especially when compared to the coding effort required to convert the GA for this one specific case. Care must be taken to avoid the y ordinate being altered during reproduction and crossover, this is achieved using a uniform crossover operator. Uniform crossover, [18], has also been found to give faster convergence than single point crossover in a μGA, [6], [19]. The population size is maintained at five. These co-ordinate values are passed to the FDTD solver which computes the resulting field distribution inside the enclosure. The peak electric field at the susceptor point is returned as the FoM to the μGA, no fitness scaling is used as tournament selection is the method of selection employed in this GA implementation, [18]. The μGA attempts to minimise this FoM, *i.e.* minimise the peak electric field at the susceptor point.

The FDTD solver is based on the equations given in [13]. The DS is one cell thick and has one cell of free space between itself and the enclosure wall. The PEC sheets are modelled as infinitely thin. A soft E_z directed sinusoidal, continuous wave, ideal Hertzian dipole of $2.05GHz$ frequency and amplitude of $10Vm^{-1}$ is used as the source in the FDTD simulation. The domain is discretised into dimensions of $7.2727mm$ in the x and z directions and $7.2mm$ in the y direction. Based on these dimensions and the material within the computational domain the time step size for the solver is set at the Courant limit, in this instance approximately $14ps$.

Initially two optimisation cases are run; a non-lossy and then a lossy dielectric slab, in the lossy case the conductivity is set to $0.04Sm^{-1}$. After this a multi-objective simulation is run where two objectives are to be optimised, these being the reduction in coupling between source and susceptor points at two specific frequencies.

5 Results

5.1 Single Objective Optimisation

The progress of the optimisation process can be seen in figure 3 where the results of both the non-lossy and lossy simulations are presented. This figure shows the evolution of the best individual in the simulation, the elite individual. While this individual remains the best the FoM remains at the same value, when a superior one is bred, a step change occurs indicating the presence of a new elite value.

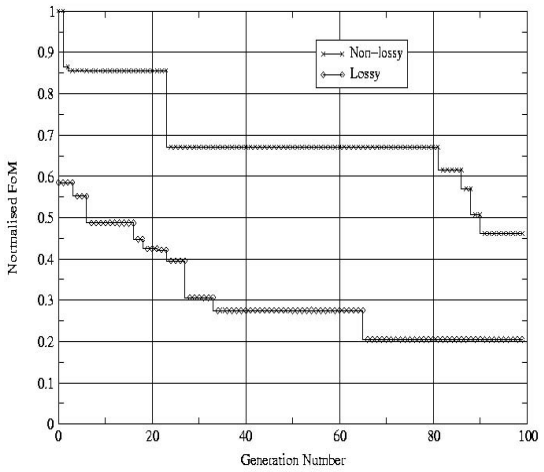

Figure 3: *Generation optimisation of both the non-lossy and lossy cases.*

The final value for the non-lossy case is $0.0541Vm^{-1}$ from an initial value of $0.1172Vm^{-1}$ and the final value for the lossy case is $0.0240Vm^{-1}$ from a value of $0.0685Vm^{-1}$. Both of the curves are normalised to the value of $0.1172Vm^{-1}$ for ease of comparison. As expected the values of field strength for the lossy case are lower than those for the non-lossy case as in the lossy case energy is dissipated in the dielectric slab. Figure 3 also shows us that the lossy case reaches its best FoM at generation 66, earlier than the non-lossy case which reaches its best FoM at generation 91. This is a random dynamic of the GA and attributable to the solution surface topology and the choice of PRNG used with the μGA. The number of generations was limited to 100 as experience with this code has shown that there is a minimal return on computing time by exceeding this point. Testimony to this is given by the fact that running the code to 200 generations gives only a final value of $0.0507Vm^{-1}$ for the non-lossy case and $0.0204Vm^{-1}$ for the lossy case, a marginal increase in performance for a doubling of computation time. This embraces one philosophy of using a GA, namely to produce an acceptable improvement toward an optimal point for a limited amount of effort.

The final field distribution on the surface of the DS can be seen in figure 4 for the non-lossy case and in figure 5 for the lossy case. These plots are generated by applying a peak hold to the E_z component at each location on the surface of the DS throughout the simulation.

The final positions of the source and susceptor points on the DS are indicated; for the non-lossy case these are at (2,16) and (3,35) respectively, and for the lossy case the co-ordinates are (2,35) and (23,11). These co-ordinate values given are of course on the x and z axes as the y ordinate is constant. These false colour plots clearly show that the μGA has indeed found good solutions but not the best solutions, the global minimum point in figure 4 is at (2,2) with a value that is $2.1dB$ down on the position found by the μGA. In figure 5 the global minimum is at (12,14) with a value that is $1.4dB$ down the μGA position. The final values found by the μGA are $57.6dB$ and $64.6dB$ down on the global maximum for the non-lossy and lossy cases respectively. It should be noted that the patterns presented in these figures are ones of over 1 million possible patterns due to source and susceptor placement, finding the global minimum on each of them would require direct evaluation of each pattern, the μGA vastly cuts down on the number of evaluations required to arrive at an acceptable result.

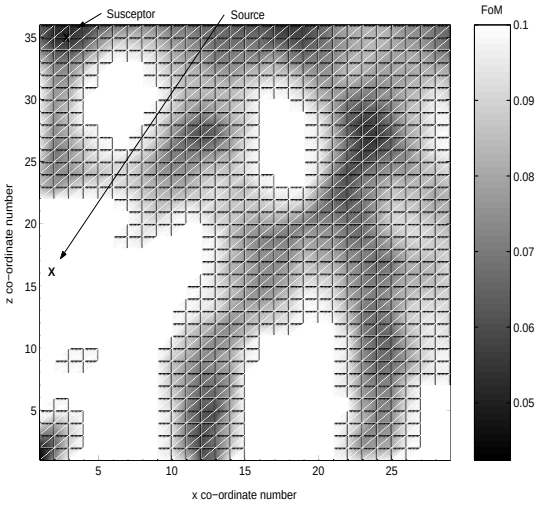

Figure 4: *False colour plot of final field distribution on surface of dielectric slab after non-lossy simulation. The x and z axes are marked in FDTD cells. Source and susceptor positions are indicated on the figure.*

5.2 Multi-objective Simulations

Multi-objective optimisation(MO) is often sought in practice as often compliance in one particular objective upsets the compliance of another objective. MO aims to achieve a solution that can not be improved upon, simultaneously, in each of the objectives. This is called a Pareto optimal solution and the set of all these solutions is called the Pareto optimal set, [20]. For the MO simulations some changes had to be made to the GA-FDTD code. As two objectives were being optimised a method of measuring their fitness at one and the same time is required, to accomplish this the method of objective weighting is used, [20]. This method is explained mathematically by equation (5),

$$Z = \sum_{i=1}^{N} w_i f_i(\boldsymbol{x}) \quad \text{where} \quad \boldsymbol{x} \in \boldsymbol{X}. \tag{5}$$

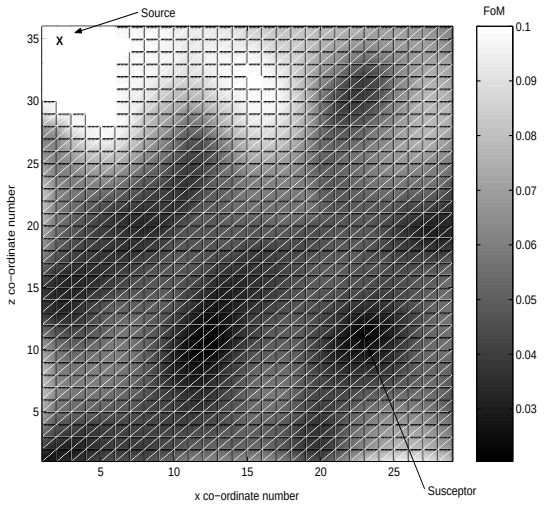

Figure 5: *False colour plot of final field distribution on surface of dielectric slab after lossy simulation. The x and z axes are marked in FDTD cells. Source and susceptor positions are indicated on the figure.*

In equation (5) Z is a scalar valued variable that is a weighted sum of the individual objectives, where there are N objectives in total. The function f is the function that returns the FoM, in this case the FDTD solver, and $\boldsymbol{x}$ represents the parameters of the function, co-ordinate values in this case. The feasible region of solutions is denoted by $\boldsymbol{X}$. The sum of the individual weights adds to 1 and each weight lies in the range 0 to 1 *i.e.* $0 \leq w_i \leq 1$. It is the scalar value Z that is optimised by the GA. The method of objective weighting is an easily implementable scheme that produces a solution from the Pareto optimal set.

The problem setup for the MO optimisation involves the same geometry as previously with the only change being the source. A Gaussian pulse modulated onto a sine wave is now used as the source. This gives a symmetrical spectrum about the carrier frequency, no DC component, and a bandwidth controlled by the length of the pulse. Its mathematical form given in [13] is described by equation (6),

$$E_z = E_0 e^{-\left[\frac{n-n_0}{n_{decay}}\right]^2} sin(2\pi f_0(n-n_0)\Delta t). \qquad (6)$$

The Gaussian pulse is centred around frequency f_0 at step n_0 with a $1/e$ characteristic decay of n_{decay} steps, and Δt is the step size. The time series and frequency response of the source is shown in figure 6. The centre frequency for the source is chosen at $1.500GHz$ and the objectives for optimisation were chosen as the minimisation of the $1.002GHz$ and $2.004GHz$ components in the frequency response which is computed on the fly as the FDTD simulation progresses as detailed in [13]. These frequencies were chosen as they tie in with equipment used in a related measurement study. Only non-lossy simulations were run in this setup.

The resulting frequency response from the E_z component at the susceptor point the simulations can be seen in figure 7. The dashed line in figure 7 shows the initial DFT before the optimisation process begins, the solid line in the figure displays the final DFT after completion of the optimisation process. A clear difference in the two curves at the respective objective frequencies can be seen. Also, it can be clearly seen that the field values at the objective frequencies, on the final DFT, are considerably lower than at other frequencies, within the same response, excepting of course at the tails of the response where there is minimal energy from the source. The values of the objectives on the final response are $54dB$ down for the $1.002GHz$ objective on the max value in the response and the value at $2.004GHz$ is $44dB$ down. Relative to the initial DFT the final response in down $27dB$ at the $1.002GHz$ objective and down $35dB$ at the $2.004GHz$ objective.

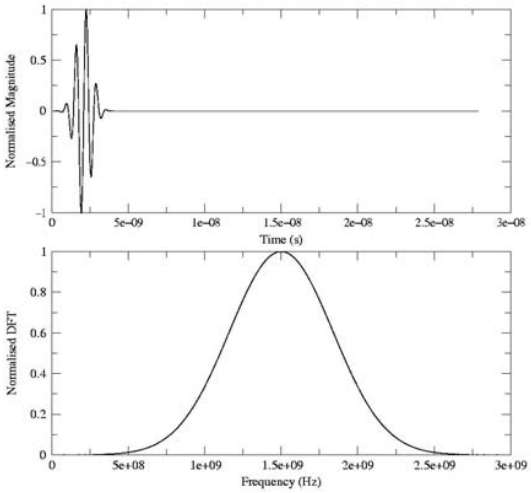

Figure 6: *Time series of the pulsed source, upper graph, and its DFT, lower graph. This is the source characteristic used in the multi-objective optimisation simulations.*

6 Conclusions

A method of using a μGA in conjunction with a FDTD solver to facilitate electromagnetic optimisation has been shown. The conjoining of the two codes allows a difficult design problem to be tackled, namely that of radiating and susceptible component placement within an arbitrary metallic structure to minimise coupling. The μGA technique is used as this gives a significant reduction in computation time with little loss in performance of the final optimised result. Ensuring that the μGA finds the global optimum in difficult optimisation problems is an area that needs further attention but the ability of the technique to reach a near optimal solution has been demonstrated. Both single and multiple objectives for optimisation have been presented with promising results from each. It is worth noting that if an exhaustive search were to be completed on the problems presented then over one million simulations would be required taking over one year to complete; the GA based search, however, took approximately four hours.

The design optimisation cases presented are rather simplistic but do prove the concept of the hybrid code. More

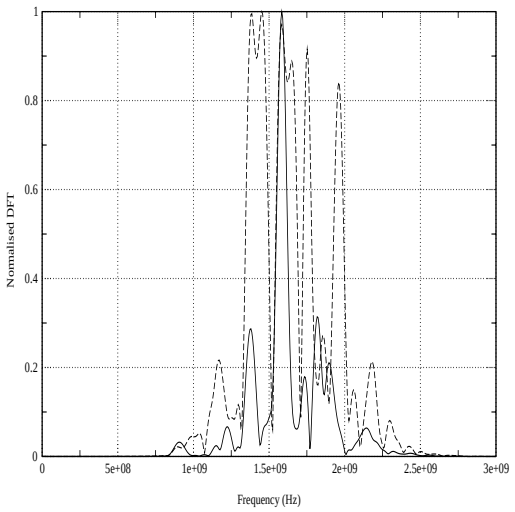

Figure 7: *DFTs of E_z at the susceptor point of the multi-objective simulation with objective of minimising the $1.002GHz$ and $2.004GHz$ frequency components of the response. Shown are the initial DFT before optimisation begins (dashed line) and the final DFT after optimisation (solid line).*

challenging problem geometries can easily be accommodated in the FDTD code with little burden to computing time as once the domain has been discretised it is the number of resulting cells that chiefly determines the computation time. It is envisaged that this tool can be used to provide design rules for component placement within an enclosed resonant cavity and that it can can also be used to assess specific designs.

References

[1] J. Mix, G. Haussmann, M. Piket-May, and K. Thomas, "EMC/EMI design and analysis using FDTD," in *IEEE Int. EMC Symp.*, vol. 1, (Denver, CO), pp. 177–181, 1998.

[2] R. I. Macpherson and N. J. Ryan, "The use of a genetic algorithm and the FDTD method for limiting resonance in shielded enclosures," in *Proceedings of EMC Europe 2000, Brugge, 4^{th} European Symposium on Electromagnetic Compatibility*, vol. 2, pp. 203–208, September 2000.

[3] D. Goldberg, *Genetic Algorithms in Search, Optimization and Machine Learning.* Reading, MA: Addison-Wesley, 1989.

[4] R. L. Haupt and S. E. Haupt, *Practical Genetic Algorithms.* John Wiley & Sons, 1998.

[5] J. Holland, *Adaption in Natural and Artificial Systems.* The University of Michigan Press, 1975.

[6] K. Krishnakumar, "Micro-genetic algorithms for stationary and non-stationary function optimization," *SPIE: Intelligent Control and Adaptive Systems*, vol. 1196, pp. 289–296, 1989.

[7] J. Jiang and G. P. Nordin, "A rigorous unidirectional method for designing finite aperture diffractive optical elements," *Optics Express*, vol. 7, no. 6, pp. 237–242, 2000.

[8] G. J. E. Rawlins, ed., *Foundations of Genetic Algorithms.* Morgan Kaufmann, 1991.

[9] D. E. Knuth, *The Art of Computer Programming*, vol. 2, Semi-numerical Algorithms. Reading, Massachusetts: Addison-Wesley, 2 ed., 1981.

[10] P. Hallekalek, "Good random number generators are (not so) easy to find," *Mathematics and Computers in Simulation*, vol. 46, pp. 485–505, 1998.

[11] P. L'Ecuyer, "Uniform random number generation," *Ann. Oper. Res.*, vol. 53, pp. 77–120, 1994.

[12] P. L'Ecuyer, *Random Number Generation.* New York: In Handbook of Simulation, Jerry Banks (ed.) Wiley, 1997.

[13] A. Taflove, *Computational Electrodynamics: The Finite-Difference Time-Domain Method.* Boston, MA: Artech House, 1995.

[14] K. S. Yee, "Numerical solution of initial boundary value problems involving Maxwell's equations in isotropic media," *IEEE Transactions on Antennas and Propagation*, vol. 14, pp. 302–307, Mar. 1966.

[15] B. Archambeault, O. M. Ramahi, and C. Brench, *EMI/EMC Computational Modeling Handbook.* Kluwer Academic Publishers, 1998.

[16] J. B. Schneider and K. Shlager, "Finite-Difference Time-Domain literature database." WWW. Available at `http://www.fdtd.org` Last Accessed 20^{th} April 2002.

[17] D. L. Carroll, "Fortran Genetic Algorithm driver." WWW. Available at `http://cuaerospace.com/carroll/ga.html` Last Accessed 20^{th} April 2002.

[18] M. Mitchell, *An Introduction to Genetic Algorithms.* MIT Press, 5 ed., 1999.

[19] D. L. Carroll, *Genetic Algorithms and Optimizing Chemical Oxygen-Iodine Lasers*, vol. XVIII of *Developments in Theoretical and Applied Mechanics*, pp. 411–424, H. Wilson, R. Batra, C. Bert, A. Davis, R. Schaper, D. Stewart, and F. Swinson eds. Guntersville, AL: The University of Alabama, 1996.

[20] N. Srinivas and K. Deb, "Multiobjective optimization using nondominated sorting in genetic algorithms," *Evolutionary Computation*, vol. 2, no. 3, pp. 221–248, 1994.

Russell Macpherson graduated with a MEng (Hons) degree in electrical and electronic engineering degree from the University of Aberdeen, Scotland, U.K. in 1999. Currently he is pursuing his PhD studies at the same institution. His research interests include genetic algorithms, artificial neural networks and fuzzy logic and how these methods can be applied to electromagnetic optimisation problems.

Nick Ryan received the BEng degree in electrical and electronic engineering from the University of Bristol, U.K. in 1990 and the PhD degree from the department of electronic and electrical engineering, University of Sheffield, U.K. in 1998. He joined the department of engineering in the University of Aberdeen, U.K. in 1997 where he currently lectures safety and reliability in electronic systems. His research interests include computational electrodynamics, electromagnetic compatibility, and renewable energy systems.